JPET Fast Forward. Published on June 4, 2014 as DOI:10.1124/jpet.114.213470

JPET #213470

Maternal-Fetal Disposition of Glyburide in Pregnant Mice Is Dependent on Gestational Age

Diana L. Shuster, Linda J. Risler, Chao-Kang J. Liang, Kenneth M. Rice, Danny D. Shen, Mary F. Hebert, Kenneth E. Thummel, and Qingcheng Mao

Department of Pharmaceutics, School of Pharmacy, University of Washington, Seattle, Washington 98195, USA (D.L.S., L.J.R., D.D.S., K.E.T., Q.M.)

Department of Biostatistics, School of Public Health, University of Washington, Seattle, Washington 98195, USA (C.J.L., K.M.R.)

Department of Pharmacy, School of Pharmacy, University of Washington, Seattle, Washington 98195, USA (M.F.H., D.D.S.)

Department of Obstetrics and Gynecology, School of Medicine, University of Washington, Seattle, Washington 98195, USA (M.F.H.)

Running Title Page: Maternal-Fetal Glyburide PK in Pregnant Mice

Corresponding Author:
Qingcheng Mao, Ph.D.
Department of Pharmaceutics
School of Pharmacy
University of Washington
Seattle, WA 98195-7610
Phone: (206) 685-0355
Fax: (206) 543-3204
Email: qmao@u.washington.edu

Number of text pages: 30 (including references, figure legends, and tables)
Number of tables: 3
Number of figures: 6 (4 Figures, 2 Supplemental Figures)
Number of references: 37
Number of words in the Abstract: 249
Number of words in the Introduction: 746
Number of words in the Discussion: 1497

Abbreviations: AUC, area under concentration-time curve; BCRP, breast cancer resistance protein; CL, clearance; CL_{int}, intrinsic clearance; CYP or *Cyp*, cytochrome P450; ER, extraction ratio; gd, gestation day; GDM, Gestational Diabetes Mellitus; GFR, glomerular filtration rate; Gly, glyburide; HPLC-MS, high performance liquid chromatography-mass spectrometry; MBRT, mean body residence time; PBS, phosphate-buffered saline; PD, pharmacodynamics; P-glycoprotein, P-gp; PK, pharmacokinetics; UGT, uridine 5'-diphospho-glucuronosyltransferase; V_c, central volume of distribution; V_β, volume of distribution at beta phase; V_{ss}, volume of distribution at steady-state; bw, body weight normalized; generalized estimating-equation (GEE).

Abstract

Gestational diabetes mellitus is a major complication of human pregnancy. The oral clearance (CL) of glyburide, an oral anti-diabetic drug, increases 2-fold in pregnant women during late gestation versus non-pregnant controls. In this study, we examined gestational age-dependent changes in maternal-fetal pharmacokinetics (PK) of glyburide and metabolites in a pregnant mouse model. Non-pregnant and pregnant FVB mice were given glyburide by retro-orbital injection. Maternal plasma was collected over 240 min on gestation days (gd) 0, 7.5, 10, 15 and 19; fetuses were colleceted on gd 15 and 19. Glyburide and metabolites were quantified using HPLC-MS, and PK analyses were performed using a pooled data bootstrap approach. Maternal CL of glyburide increased ~2-fold on gd 10, 15, and 19 compared to non-pregnant controls. CL_{int} of glyburide in maternal liver microsomes also increased as gestation progressed. Maternal metabolite/glyburide AUC ratios were generally unchanged or slightly decreased throughout gestation. Total fetal exposure to glyburide was < 5% of maternal plasma exposure, and was doubled on gd 19 versus gd 15. Fetal metabolite concentrations were below the limit of assay detection. This is the first evidence of gestational age-dependent changes in glyburide PK. Increased maternal glyburide clearance during gestation is attributable to increased hepatic metabolism. Metabolite elimination may also increase during pregnancy. In the mouse model, fetal exposure to glyburide is gestational age-dependent and low compared to maternal plasma exposure. These results indicate that maternal glyburide therapeutic strategies may require adjustments in a gestational-age dependent manner if these same changes occur in humans.

Introduction

Gestational diabetes mellitus (GDM) complicates 5-14% of human pregnancies (Jovanovic and Pettitt, 2001; Paglia and Coustan, 2011). Like Type-2 diabetes, the pathology of GDM is a combination of increased insulin resistance and decreased insulin sensitivity. If left untreated, GDM poses significant risks to the mother, fetus, and neonate. Such risks include maternal hypertension, preeclampsia, and cesarean delivery, as well as fetal/neonatal morbidities including macrosomia, hypoglycemia, as well as increased risk of metabolic syndrome, Type-2 diabetes, and obesity for the offspring later in life (2001; 2002). While insulin resistance occurs in normal pregnancy, women with GDM experience insulin resistance beyond their ability to compensate with increased insulin production, leading to hyperglycemia. Although insulin has been the standard of care for pharmacotherapeutic treatment of GDM, oral anti-diabetic agents such as glyburide have gained increasing popularity because of their ease of administration, lower cost, and comparable efficacy to insulin (Langer et al., 2000).

Diagnosis of GDM generally takes place during the second trimester of pregnancy. It has been well established that physiological, biochemical, and hormonal changes during pregnancy can alter the pharmacokinetics (PK) of drugs throughout gestation (e.g., increased hepatic blood flow and glomerular filtration, and/or changes in the expression of drug-metabolizing enzymes and transporters) (Klieger et al., 2009). However, data is quite limited regarding the PK of glyburide during pregnancy, particularly in relation to gestational age. One study estimated a 2-fold increase in the oral clearance of glyburide in women with GDM in the third trimester of pregnancy compared to non-pregnant women with Type-2 Diabetes Mellitus (Hebert et al., 2009). Formation clearance of 4-*trans*-hydroxycyclohexyl glyburide (M1), a pharmacologically active metabolite, was also increased more than 2-fold in the GDM group. Glyburide crosses

human placenta, but at a much slower rate compared to the placental transfer marker antipyrine (Nanovskaya et al., 2006), which was not expected given the low molecular weight and high lipophilicity of glyburide. This low rate of placental transfer could be explained by extremely high plasma protein binding of glyburide (Nanovskaya et al., 2006) and efflux transport at the apical membrane of the syncytiotrophoblasts in humans and mice. The ATP-Binding Cassette (ABC) transporters breast cancer resistance protein (BCRP) and P-glycoprotein (P-gp) have been implicated as placental barriers to glyburide (Gedeon et al., 2006; Gedeon et al., 2008b; Zhou et al., 2008; Hemauer et al., 2010). Although multidrug resistance proteins (MRP1 and MRP3) also transport glyburide (Gedeon et al., 2006; Hemauer et al., 2010), human placenta perfusion studies suggest that MRPs may only play a minor role in the transport of glyburide across human placenta (Gedeon et al., 2008a). The time-course and mechanism by which pregnancy changes glyburide PK throughout gestation remain largely unexplained. Therefore, the main objective of this study was to investigate gestational age-dependent changes in maternal-fetal disposition of glyburide and the mechanisms behind these changes.

Since hepatic CYP3A and CYP2C9 activities are significantly induced during pregnancy (Hebert et al., 2008; Feghali and Mattison, 2011), CYP induction could be one possible mechanism for the increased maternal glyburide clearance during pregnancy. Like in humans, glyburide clearance in pregnant mice was similarly doubled on gestation day (gd) 15 compared to non-pregnant controls (Zhou et al., 2010b), suggesting that the pregnant mouse may be an appropriate animal model to study glyburide PK during pregnancy. The mRNA levels of several hepatic *Cyp3a* isoforms and CYP3A activity in pregnant mice are significantly increased in a gestational age-dependent manner compared with non-pregnant controls (Zhang et al., 2008;

Shuster et al., 2013). Therefore, we used pregnant mice to study gestational age-dependent effects on maternal-fetal disposition of glyburide.

In vitro microsomal incubation studies suggest that glyburide is extensively metabolized in the liver by CYP3A4, CYP2C9, and CYP2C19 to six major metabolites: 4-*trans*-hydroxycyclohexyl glyburide (M1), 4-*cis*-hydroxycyclohexyl glyburide (M2a), 3-*cis*-hydroxycyclohexyl glyburide (M2b), 3-*trans*-hydroxycyclohexyl glyburide (M3), 2-*trans*-hydroxycyclohexyl glyburide (M4), and ethylene-hydroxylated glyburide (M5) (Ravindran et al., 2006; Zharikova et al., 2009). Because M1 and M2b are potentially pharmacologically active (Rydberg et al., 1994) and limited data exists regarding metabolite PK in pregnant and non-pregnant individuals, we also examined maternal-fetal disposition of metabolites.

In the present study, we first determined maternal-fetal PK of glyburide and its metabolites throughout gestation in pregnant mice. We then investigated whether the intrinsic clearance of glyburide in microsomes isolated from the livers of pregnant mice was increased in a gestational age-dependent manner. The data obtained in this study will facilitate mechanistic understanding of changes in maternal-fetal PK of glyburide and its metabolites throughout gestation, which is imperative for gestational age-dependent therapeutic strategies.

Methods

Materials. Glyburide (Gly) and glipizide were purchased from Sigma-Aldrich (St. Louis, MO). Glyburide metabolites: 4-*trans*-hydroxycyclohexyl glyburide (M1), 4-*cis*-hydroxycyclohexyl glyburide (M2a), 3-*cis*-hydroxycyclohexyl glyburide (M2b), and 3-*trans*-hydroxycyclohexyl glyburide (M3) were purchased from Toronto Research Chemicals (Toronto, Ontario, Canada). 2-*Trans*-hydroxycyclohexyl glyburide (M4), and ethylene-hydroxylated

glyburide (M5) are not commercially available, and therefore were not included in our metabolite analyses. Internal standards glyburide-*d11* and 4-*trans*-hydroxycyclohexyl glyburide-*d3,13C* were also purchased from Toronto Research Chemicals. [Cyclohexyl-2,3-^{3}H(N)]-glyburide ([^{3}H]-Gly) (50 Ci/mmol) was obtained from PerkinElmer Life (Waltham, MA). β-nicotinamide adenine dinucleotide 2′-phosphate reduced (NADPH) tetrasodium salt hydrate, potassium phosphate monobasic (KH_2PO_4), and ethylenediaminetetraacetic acid (EDTA) were purchased from Sigma-Aldrich. Optima-grade (or HPLC grade) methanol, dimethyl sulfoxide, polyethylene glycol 400, ethanol, *n*-hexane, methylene chloride, formic acid, ammonium formate and water were obtained from Thermo Fisher Scientific (Waltham, MA) or Acros Organics (Pittsburgh, PA). Phosphate-buffered saline (PBS) was purchased from Corning Cellgro (Manassas, VA).

Animal studies. Wild-type FVB mice, 7-10 weeks of age, were purchased from Taconic Farms (Germantown, NY) and cared for in accordance with the Guide for the Care and Use of Laboratory Animals published by the National Research Council. The animal protocol for this study was approved by the Institutional Animal Care and Use Committee at the University of Washington. Briefly, mice were maintained under 12-hour light/dark cycles, and food was provided *ad libitum*. Female mice, 7-10 weeks of age, were mated with male mice of the same age overnight using a female to male ratio of 2:1. Gestation day (gd) 1 was defined as the presence of a sperm plug following overnight housing; non-pregnant mice were defined as gd 0. Progression of pregnancy was monitored by visual inspection and body weight increase. Body weight was recorded on the day of dosing.

Glyburide was dissolved in 0.5 % (v/v) dimethyl sulfoxide, 10% (v/v) ethanol, 39.5% (v/v) saline, and 50% (v/v) polyethylene glycol 400 at a concentration of 0.5 mg/ml. Under

anesthesia (2-5% isoflurane), pregnant (gd 7.5, 10, 15, and 19) or non-pregnant (gd 0) mice were administered 20 µg glyburide per mouse by retro-orbital injection (40 µl each injection). The 20 µg dose was selected to achieve maternal plasma concentrations in the 10-1,000 ng/ml range which is comparable to steady-state plasma concentrations observed in pregnant women during the third trimester of pregnancy, as we demonstrated in previous studies with pregnant and non-pregnant mice receiving a glyburide dose of 1 mg/kg body weight (Zhou et al., 2008; Hebert et al., 2009; Zhou et al., 2010b). The same dose of glyburide (20 µg) was used across gestational ages because the increase in body weight during pregnancy is mainly due to the presence of placenta and fetuses, which do not significantly contribute to the overall distribution volume and metabolic clearance of glyburide. Additionally, in clinical practice, glyburide is not administered based on body weight, therefore maintaining the same dose across gestation better mimics clinical scenarios. Depth of anesthesia was evaluated using the front-toe pinch method. At various times (0.5, 5, 10, 20, 40, 60, 120, 180, and 240 min) after glyburide administration, animals (n = 3-5 per time point) were sacrificed under anesthesia by cardiac puncture (i.e., a total of ~30 samples for each gd). Maternal blood was collected in heparinized microcentrifuge tubes (BD Biosciences, San Jose, CA) and centrifuged at 1,000 × g for 10 minutes at 4°C. Plasma was collected and stored at -80°C until further analysis. Individual whole fetuses were collected from mice dosed on gd 15 and 19. Maternal mouse livers were also collected (n = 5-6 per gd) for microsomal preparation from mice that had not been dosed with glyburide. Tissues were immediately rinsed with phosphate-buffered saline (PBS), snap-frozen in liquid nitrogen, and stored at -80°C until use.

Quantification of glyburide and metabolites in maternal plasma and fetal homogenates. Glyburide and metabolite quantification in maternal plasma and fetal

homogenates was performed using a previously validated HPLC-MS method with some modifications (Naraharisetti et al., 2007). Most notable was the use of protein precipitation for the isolation of glyburide and metabolites from maternal plasma and fetal homogenates in place of liquid-liquid extraction. In brief, for every 100 µl of maternal plasma, 450 µl of methanol and 20 µl of working internal standards (0.5 ng/µl glyburide-*d11* and 0.15 ng/µl 4-*trans*-hydroxycyclohexyl glyburide-*d3,13C*) were added into a 1.5 ml microcentrifuge tube. Plasma samples were briefly vortexed and centrifuged at 20,800 × g for 10 min at 4°C. Supernatants were transferred to disposable clean glass tubes and evaporated using nitrogen gas. Samples were reconstituted in 75 µl initial mobile phase and 2 µl were injected per sample for HPLC-MS analysis. A calibration curve was prepared identically using human plasma as a matrix with a dynamic range of 10-4,000 ng/ml for glyburide and 1.2-120 ng/ml for M1-M3.

Individual whole fetuses were homogenized in 1.5-2.5 ml of PBS using an Omni Bead Ruptor Homogenizer (Omni International, Kennesaw, GA). For every 500 µl of fetal homogenates, 50 µl of 2 M HCl, 4 mL of 60/40 (v/v) *n*-hexane/methylene chloride, and 20 µl of working internal standard (0.5 ng/µl glyburide-*d11*) were added in a 13 × 100-mm borosilicate glass culture tube. Fetal samples were vortexed 30 s and centrifuged at 1,970 × g for 10 min at 4°C. Supernatants were transferred to disposable clean glass tubes and evaporated using nitrogen gas. Each sample was reconstituted in 75 µl of 1% formic acid in methanol and 2 µl were injected per sample for HPLC-MS analysis. A calibration curve for glyburide was prepared using 500 µl of blank fetal homogenate (matched by gestational age) as matrix, over a dynamic range of 0.05-2 ng glyburide. Calibration according to analyte amount was chosen for fetal tissue analysis to accommodate the variations in fetal tissue specimen size and homogenate dilutions. No matrix effect was observed; i.e., glyburide extraction recovery and instrument response did

not vary over the range of fetal homogenate concentrations prepared on samples taken from gd 15 and 19 (0.06-0.6 g fetus/ml PBS).

The previously validated HPLC-MS method did not include M2a and M3 for lack of commercially available standards at the time (Naraharisetti et al., 2007). Those standards are now available; therefore, we modified the above method slightly to incorporate the separation and quantification of M1-M3 in maternal plasma. These metabolites were quantifiable in maternal plasma, but not detectable in fetal tissue samples.

In brief, HPLC-MS was performed using an Agilent series 1100 HPLC interfaced with an Agilent G1956B single quadrupole mass spectrometer (Agilent Technologies, Palo Alto, CA). Separation of glyburide and all metabolites in maternal plasma and fetal homogenates was achieved using an Ace 3 C8 column (150 mm × 2.1 mm, 3 micron) with gradient elution. The mobile phases consisted of methanol containing 5 mM ammonium formate (B) and water containing 5 mM ammonium formate at pH 6.0 (A). The flow rate was set to 0.4 ml/min. The gradient was 42.5% methanol for the first 5 min, then increased linearly to 90% for 5.1 min, and finally decreased back to 42.5% for the remainder of the 11-min run time. The mass spectrometer was run in API-ES positive ionization mode with a capillary voltage of 3500 V and a fragmentation voltage of 90 V for M1-M3 and *trans*-4-hydroxy glyburide-*d3,13C* or 115 V for glyburide and glyburide-*d11*. The drying gas temperature was 350ºC, the nitrogen drying gas flow rate was 12 L/min, and the nebulizer pressure was 35 pound-force per square-inch-gauge. Ions monitored were 494 *m*/z for glyburide, 505 *m*/z for glyburide-*d11*, 510 *m*/z for M1-M3, and 514 *m*/z *trans*-4-hydroxy glyburide *d3,13C.* Select ion chromatograms generated from sample extracts and that demonstrate the separation of glyburide and metabolites are presented as supplemental data (Supplemental Figure 1). The lower limit of quantification in maternal plasma

was 10 ng/ml for glyburide and 1.2 ng/ml for M1-M3 (Supplemental Figure 2). Blank human plasma spiked with glyburide and metabolites was used for quality control samples for maternal plasma and fetal homogenate analyses. Inter- and intra-day variability of glyburide and metabolites were less than 5% and 2%, respectively.

Plasma protein binding. Mouse plasma protein binding was determined by ultrafiltration using Microcon-10 kDa Centrifugal Filters with Ultracel-10 membranes (EMD Millipore Corporation, Billerica, MA). [^{3}H]-Glyburide (1 ng) in methanol was aliquoted into 1.5 ml eppendorf tubes and evaporated to dryness. Maternal plasma collected after glyburide administration on gd 0, 7.5, 10, 15 and 19 was added to each tube to a total volume of 220 µl. Samples were briefly vortexed and allowed to equilibrate for 30 min at 37°C. Two 100 µl aliquots from each sample were transferred to ultrafiltration cartridges, equilibrated for 30 min at 37°C, and centrifuged at 1,000 × g for 10 min. Eight microliters of filtrate and unfiltered plasma were counted on a liquid scintillation counter. The fraction unbound (f_u) of glyburide was calculated as the percentage of radioactivity of the filtrate to the radioactivity of the corresponding unfiltered plasma. Non-specific binding of [^{3}H]-Gly was determined using PBS rather than plasma, and was 15.8 ± 4.8% (n = 5 determinations done in duplicate).

Glyburide depletion kinetics in maternal mouse liver microsomes. Microsomes were prepared from individual maternal mouse livers (n = 5-6 per gd) as previously described (Thummel et al., 1993; Paine et al., 1997). Briefly, approximately 1 g of mouse liver tissue was homogenized in 3 ml of homogenization buffer (50 mM KPi buffer containing 0.25 M sucrose and 1 mM EDTA) using an Omni Bead Ruptor Homogenizer (Omni International, Kennesaw, GA). The homogenate was centrifuged at 15,000 × g for 30 min at 4°C, and the supernatant at 120,000 × g for 70 min at 4°C. Microsomal pellets were carefully resuspended in washing buffer

(10 mM KPi, 0.1 mM KCl, and 1 mM EDTA, pH 7.4) and centrifuged again at 120,000 × g for 70 min at 4°C. Microsomal pellets were finally resuspended in 1 ml of storage buffer (50 mM KPi, 0.25 M sucrose, and 10 mM EDTA, pH 7.4), and stored at -80°C until use. Microsomal protein concentrations were determined using the Pierce BCA Protein Assay Kit (Thermo Scientific, Rockford, IL) with bovine serum albumin as the standard.

Glyburide depletion reaction mixtures contained 0.3 mg/ml microsomal protein and 0.5 µM glyburide (dissolved in <1% v/v methanol) in 200 µl of 100 mM KH_2PO_4 buffer (1 mM EDTA, pH 7.4). The concentration of glyburide selected was below the K_m values of CYP3A4 and CYP3A5 for glyburide depletion, which are both reported to be ~5 µM (Zhou et al., 2010a). After pre-incubating for 5 min, reactions were initiated by adding NADPH to a final concentration of 1 mM. Incubations without NADPH were used as negative controls. Reactions were stopped at 0, 3, 6, 10, 15, 20, and 30 min with 200 µl of ice-cold methanol. Following the addition of 20 µl of glipizide (internal standard, 1 ng/µl), samples were briefly vortexed and centrifuged at 20,800 × g for 10 min at 4°C. The supernatant was transferred to a 96-well plate and 1 µl was injected for analysis by HPLC-MS. Glyburide concentration remaining at the various time points was analyzed graphically on a semilogarithmic plot. The first-order rate constant for glyburide depletion (k_{dep}, min^{-1}) was estimated by least-squares regression of the log-linear portion of the depletion curve. The intrinsic clearance (CL_{int}) was calculated using the following equation:

CL_{int} = [k_{dep} × incubation volume in ml]/amount of microsomal protein in mg

Statistically significant differences of CL_{int} between gd 0 and other gestation days were determined using the Kruskal-Wallis test followed by the Dunn's Multiple Comparison test assuming a significance level of 0.05.

Quantification of glyburide in mouse liver microsomes. Chromatographic separation of glyburide in extracts of mouse liver microsomal incubates was achieved using an Agilent Extend C18 column (50 mm × 2.1 mm, 5 micron) with gradient elution. The mobile phases consisted of methanol (B) and water containing 0.1% formic acid (A). The flow rate was set to 0.4 ml/min. The gradient was 30% methanol for the first 2 min, increased linearly to 75% for 3 min, held for 1 min at 75% methanol, and finally decreased back to 30% for the remainder of the 9-min run time. The mass spectrometer was run in API-ES positive ionization mode with a capillary voltage of 3500 V and a fragmentation voltage of 90 V for glyburide and glipizide. The drying gas temperature was 350ºC, the nitrogen drying gas flow rate was 10 L/min, and the nebulizer pressure was 35 pound-force per square-inch-gauge. Ions monitored were 494 *m*/z for glyburide and 446 *m*/z for glipizide.

Pharmacokinetic and statistical analysis of glyburide and metabolites in pregnant mice. Maternal PK parameters were estimated for each gd using a pooled data bootstrap method as previously described (Mager and Goller, 1998) with some modifications. Briefly, the following steps were used to obtain PK parameter estimates: 1) Concentration-time points from one gd group were sampled randomly with replacement 30 times using R programming software (R Core Team, 2014); 2) A two-compartment model was fit to the bootstrapped pseudo concentration-time profiles using the following equation and upper constraint: $C_t = Ae^{-\alpha t} + Be^{-\beta t}$, ($A+B \leq 12{,}500$ ng·ml^{-1}), where C_t is the plasma concentration at time *t* after dosing. The upper constraint for the sum of A and B was set to the highest possible blood concentration of glyburide in a 20 g female mouse given a 20 μg retro-orbital dose, i.e., 20 μg distributed in a blood volume of 1.6 ml or 8% of mouse total body weight; 3) A, B, α, β and average body weight of mice in the given pseudo-profile were used to calculate $AUC_{0\text{-}240\ min}$, CL with and

without body weight normalization (CL and CL_{bw}), central volume of distribution with and without body weight normalization (V_c and $V_{c, bw}$), volume of distribution at steady-state or beta phase with and without body weight normalization (V_{ss} and $V_{ss, bw}$ or V_β and $V_{\beta, bw}$), and mean body residence time (MBRT). The average body weight of the mice used to generate the pseudo-profile was used to calculate body weight normalized estimates of clearance and volume of distribution; 4) Steps 1-3 were repeated 10,000 times to create a distribution of PK parameter estimates; 5) Based on the distribution of PK parameter estimates, 95% confidence intervals were obtained for all PK parameters. The above five steps were repeated for all gd groups. To determine whether PK parameters for pregnant mice (gd 7.5, 10, 15, and 19) were significantly different from those of non-pregnant mice (gd 0), we calculated two-sided *p*-values using permutation tests with 10,000 replications (Westfall and Young, 1993). If the *p*-value was less than 0.05, the difference was considered to be statistically significant.

Maternal metabolite AUCs for each gd group and fetal glyburide AUCs for gd 15 and 19 were estimated using the same bootstrapping method as described above. Fetal glyburide concentrations were determined in individual fetuses and averaged by litter prior to bootstrap analysis. Due to the complexity of maternal metabolite kinetics and fetal glyburide kinetics, only non-compartmental analyses were feasible. We chose to estimate AUCs using the linear trapezoidal rule. To evaluate if compartmental and non-compartmental approaches produce comparable results, the AUCs of glyburide in maternal plasma were estimated using non-compartmental analysis as well. This allowed calculations of the maternal metabolite to glyburide AUC ratios as well as the fetal to maternal glyburide AUC ratios. Statistical significance between maternal metabolite AUCs and metabolite to glyburide AUC ratios estimated on gd 7.5, 10, 15 or 19 versus gd 0 were determined as described in the above

paragraph. Likewise, statistical comparisons of fetal glyburide AUCs or AUC ratios between gd 15 and 19 were conducted using the same method.

Differences in fetal glyburide concentrations were compared between gd 15 and 19 at each of nine time points (from 0 to 240 minutes) and evaluated for statistical significance. Because glyburide was quantified in individual fetuses, fetal concentrations derived from the same litter were not considered statistically independent. For that reason, a generalized-estimating-equation (GEE) approach was used to account for that dependence. Differences in fetal glyburide concentrations between gd 15 and 19 at each time point (between 0 and 240 minutes) were therefore determined using GEE with an independent correlation structure. The same approach was used to model differences between fetal-maternal glyburide concentration ratios on gd 15 and 19 at each time point. In both cases, the R package geepack (Yan and Fine, 2004; Halekoh et al., 2006) was used to perform the calculations, and calculated *p*-values were adjusted for multiple testing using a Bonferroni correction.

Results

Maternal glyburide disposition changed in a gestational age-dependent manner. Wild-type FVB mice of various gestational ages (gd 0, 7.5, 10, 15 and 19) were administered 20 µg glyburide per mouse by retro-orbital injection. As shown in Figure 1, within each gd group, maternal plasma glyburide concentrations decreased over time from 0 to 240 min in a biexponential fashion. As gestation advanced, glyburide concentrations showed progressive decrease at nearly every time point; the largest differences between gestational ages occurred in the first 60 min after dosing. These changes are reflected by decreases in the coefficient of the slow exponential term (B) when the bootstrapped plasma concentration data were fit to a

biexponetnial equation. However, distribution (α) and elimination (β) rate constants remained unchanged during pregnancy (Table 1). All the derived two-compartmental model parameters for the maternal plasma glyburide PK are shown in Table 1. The $AUC_{0\text{-}240\ min}$ of glyburide steadily decreased throughout gestation by as much as 50% on gd 15 and 19 compared to non-pregnant controls (20.7, 21.2, and 47.9 $\mu g \cdot min \cdot ml^{-1}$on gd 15, 19, and 0, respectively; $p = 0.001$). Accordingly, glyburide CL increased more than 2-fold on gd 15 and 19 compared to non-pregnant controls (0.97, 0.94, and 0.42 $ml \cdot min^{-1}$ on gd 15, 19, and 0, respectively; $p < 0.05$). Body weight normalized estimates of CL (CL_{bw}) also demonstrated a gestational age-dependent increase (~1.5-fold increase on gd 15 and 19 versus gd 0). V_c was unaffected by pregnancy; however, V_β and V_{ss} showed a significant 2-fold increase on gd 10 and nearly tripled on gd 15 and 19 compared to non-pregnant controls. MBRT did not significantly change throughout gestation since the distribution and elimination rate constants did not vary across gestational ages. Maternal plasma protein binding (f_u) of glyburide was not significantly affected by pregnancy throughout gestation.

Maternal metabolite exposure relative to glyburide exposure was unchanged during pregnancy. Primary metabolites of glyburide, M1, M2a, M2b and M3, were also quantified in all maternal plasma samples collected. As shown in Figure 2, within each gd group, maternal plasma concentrations of all four metabolites first increased to a maximum at times around 30-60 min and then decreased over time to 240 min. The concentrations of all four metabolites (0-4 $ng \cdot ml^{-1}$) were approximately 1,000 times lower compared to those of glyburide (10-6,000 $ng \cdot ml^{-1}$). Similar to glyburide, metabolite concentrations at most time points tended to decrease as gestation progressed; however, the differences in metabolite concentrations and $AUC_{0\text{-}240\ min}$ estimates compared to non-pregnant controls were greatest on gd 15 and slightly reversed on gd

19 (rather than the sustained increase on gd 15 and 19 in the case of glyburide). Indeed, $AUC_{0\text{-}240\ min}$ for M1 significantly decreased by 200% on gd 15 and 150% on gd 19 compared to gd 0 (129 and 141 ng·min·ml^{-1} compared to 251 ng·min·ml^{-1}, respectively) (Table 2). $AUC_{0\text{-}240\ min}$ of M2a, M2b, and M3 all decreased by 300% on gd 15 compared to gd 0 (Table 2). Though the metabolite to glyburide AUC ratios for M1 and M2a on gd 10 or for M2b and M3 on gd 15 were significantly increased or decreased, respectively, these ratios were <1% for all metabolites across all gestational ages. Maternal plasma AUCs of glyburide estimated using non-compartmental analysis shown in Table 2 were comparable to those calculated using a two-compartmental model shown in Table 1.

Fetal exposure to glyburide doubled from mid to late gestation. On gd 15 and 19, individual fetuses were collected simultaneously to determine fetal exposure to glyburide and metabolites. Concentrations of glyburide in fetal homogenates ranged from ~1-10 ng·g^{-1} fetus, and were lower overall on gd 15 compared to gd 19 (Figure 3A). The fetal-to-maternal plasma concentration ratios of glyburide on gd 19 were also generally greater than those on gd 15 at several time points from 0.5 to 240 min (Figure 3B). Consequently, the fetal $AUC_{0\text{-}240\ min}$ of glyburide on gd 19 was significantly increased 2-fold compared to gd 15 (905 versus 462 ng·min·g^{-1}, respectively; $p < 0.001$) (Table 3). The fetal-to-maternal plasma $AUC_{0\text{-}240\ min}$ ratio of glyburide doubled from gd 15 to 19 as well (1.8% versus 3.7%, respectively; $p = 0.007$). Fetal concentrations of all four metabolites were below the detection limit for all time points on gd 15 and 19.

Gestational age-dependent changes in maternal glyburide metabolism. We hypothesized that increased glyburide CL in pregnant mice versus non-pregnant controls is the result of increased CYP-mediated metabolism of glyburide in the liver. To test this hypothesis,

glyburide depletion rate was measured in microsomes prepared from maternal livers collected on gd 0, 7.5, 10, 15 and 19. Mean time courses of glyburide depletion during incubation with liver microsomes for the five gestational age groups are shown in Figure 4A. There was indeed a gestational age-dependent increase in glyburide CL_{int} in the liver, which doubled by gd 19 versus gd 0 (0.17 versus 0.09 ml·min^{-1}·mg protein^{-1}, respectively) (Figure 4B).

Discussion

Previous clinical studies showed that the oral clearance of glyburide increased 2-fold during the third trimester in pregnant women with GDM compared to non-pregnant controls (Hebert et al., 2009). Diagnosis and treatment of GDM most often occur in the second trimester (Metzger et al., 2007). In addition, women at risk for developing GDM or with a previous history of GDM may be screened and treated earlier in pregnancy (Metzger et al., 2007). Therefore, it is important to understand glyburide PK changes throughout gestation, and how such changes affect glycemic control. In this study, we characterized maternal-fetal glyburide disposition throughout gestation in a pregnant mouse model, since it is not feasible to obtain data at this level of detail in pregnant women.

We found that the maternal plasma PK of glyburide changes in a gestational age-dependent manner, with the largest alterations occurring in mid-late gestation on gd 15 and 19 (Figure 1 and Table 1). In particular, maternal glyburide CL, V_{β}, and V_{ss} steadily increased over gestation and were approximately doubled by mid-late gestation. Glyburide is a low hepatic ER drug (ER = ~0.1) with no significant renal CL. Therefore, the increase in maternal systemic CL could be accounted for by changes in fraction unbound in plasma and CL_{int} of glyburide in the liver. The fraction unbound (f_u) did not increase throughout gestation (Table 1), which was

somewhat unexpected, considering that plasma albumin is known to decrease during pregnancy (Anderson, 2005). However, the f_u of glyburide also did not change in pregnant women with GDM compared to non-pregnant controls (Hebert et al., 2009). The reasons why the f_u was unaffected by pregnancy are not clear. It is possible that glyburide can bind to other lipoproteins in the plasma and/or there are biochemical changes in maternal plasma that have offsetting modulation on plasma protein binding of glyburide. Since the f_u of glyburide in maternal plasma did not significantly change throughout gestation, the increase in maternal glyburide CL and CL_{bw} is most likely caused by an increase in hepatic CL_{int}. Indeed, the glyburide depletion rate in mouse liver microsomes steadily increased as gestation progressed (Figure 4). Using ketoconazole as a CYP3A inhibitor, we previously showed that glyburide was primarily metabolized by CYP3A in mouse liver (Zhou et al., 2010b). This is consistent with the finding that hepatic CYP3A activity is significantly induced by pregnancy both in humans and mice (Hebert et al., 2008; Zhang et al., 2008). The present study further confirmed that hepatic CYP3A activity in pregnant mice is induced in a gestational age-dependent manner. It is not known which mouse CYP3A isoforms are responsible for increased glyburide metabolism during pregnancy as we and others have shown that mRNA levels of *Cyp3a16, Cyp3a41,* and *Cyp3a44* are induced, while *Cyp3a11, Cyp3a13,* and *Cyp3a25* genes are down-regulated in a gestational age-dependent manner (Zhang et al., 2008; Shuster et al., 2013). Increases in V_{ss} and V_{β} most likely reflect increases in total body water and fat content during pregnancy, and further suggest that distribution of glyburide into maternal tissues is increased during pregnancy.

Although the pharmacodynamics and therapeutic window of glyburide have not been well characterized, it is possible that 1.5-2-fold increases in glyburide CL (and CL_{bw}) and corresponding decreases in AUC warrant consideration when determining appropriate

therapeutic management of glyburide in pregnant women. If our animal data indeed reflect gestational age-dependent changes in maternal glyburide CL and AUC in humans, dosing adjustments may be required as early as the first or second trimester. This would be particularly important for pregnant women treated with glyburide starting in the first or second trimester.

Understanding maternal disposition of primary metabolites of glyburide is also important as some metabolites (e.g. M1 and M2b) are pharmacologically active (Balant et al., 1979; Rydberg et al., 1994). We had expected that increased glyburide CL across gestation would lead to either no change or increase in formation of M1-M3, if they are all derived from pathways that are up-regulated; instead, maternal plasma AUCs of each of the measured metabolites decreased progressively reaching a nadir by gd 15 and slightly reversed by gd 19 (Figure 2 and Table 2).

AUC of a metabolite represents the balance of its formation and elimination rates. A decrease in metabolite AUC can possibly be explained by an increase in elimination clearance of the metabolite. Accelerated metabolite elimination could be due to increased secondary oxidative metabolism, increased Phase II conjugation, and/or increased renal clearance of the metabolites. In humans, M1 undergoes glucuronidation mediated by uridine 5'-diphospho-glucuronosyltransferases (UGTs) and M2b is excreted unchanged in the urine (Naraharisetti et al., 2007). UGT1A1 and UGT1A4 expression is indeed induced during human pregnancy (Feghali and Mattison, 2011); however, mRNA levels of UGTs in pregnant mice are relatively unchanged (Shuster et al., 2013). Mechanisms of renal clearance (i.e. active tubular secretion and/or reabsorption) remain unknown for all glyburide metabolites in humans and mice. Further investigation is required to elucidate the mechanisms of the putative increase in metabolite elimination.

Another possible explanation for a decrease in metabolite AUC as gestation progresses is that the increase in glyburide CL is due to an increase in normally minor metabolic pathway(s) not represented by the measured metabolites; that is, up-regulation of competing pathway(s) resulting in a decrease in formation of the measured metabolites. M1, M2a, M2b, M3, M4 and M5 are the primary metabolites of glyburide produced by the human liver, and glyburide is metabolized primarily to M5 in human placenta by CYP19 (Zharikova et al., 2009). It is therefore possible that decreases in concentrations of M1-M3 could be due to increased formation of M4 and/or M5 in maternal liver and placenta. However, without commercially available standards for M4 and M5, we were unable to quantify gestational age-dependent changes in maternal concentrations of M4 and M5.

Table 2 also presents the metabolite-to-glyburide AUC ratio, which is governed by the ratio of a given metabolite's formation clearance to its elimination clearance. It is a quantitative index reflecting either the joint or opposing effects of simultaneous changes in formation and elimination clearances of a primary metabolite. Mean AUC ratios for M1and M2a were elevated on gd 10 and declined to near the gd 0 values by gd 15 and 19. This suggests that the increase in formation clearance of these two metabolites outpaced the increase in their elimination clearances by gd 10; moreover, the changes in formation and elimination clearances became comparable as gestation progressed beyond gd 10. For M2b and M3, their AUC ratios declined across all the gestation days studied, suggesting that there was a greater increase in elimination clearance compared to formation clearance.

Fetal exposure to glyburide was <5% of maternal exposure, but was doubled on gd 19 versus gd 15 (Table 3 and Figure 3). This change is consistent with the finding that protein expression of BCRP in mouse placenta on gd 15 is 2-3 times greater than that on gd 19 (Wang et

al., 2006). Glyburide is a substrate of mouse and human BCRP, which limit the transport of glyburide across the placenta barrier (Gedeon et al., 2006; Zhou et al., 2008; Hemauer et al., 2010). As BCRP protein expression decreases from gd 15 to gd 19, glyburide penetration across the placenta to the fetus increases. P-gp could also contribute to the gestational age-dependent changes in fetal exposure to glyburide because both human and mouse P-gp expression in the placenta decreases as gestation progresses (Mathias et al., 2005; Aleksunes et al., 2008; Zhang et al., 2008). M1-M3 were not detectable in fetal homogenates, suggesting that fetal exposure to these primary metabolites is negligible due to their low concentrations in maternal circulations. Since glyburide is highly bound to plasma proteins with a low volume of distribution, the actual fetal plasma concentrations may be higher than what we observed in fetal homogenates. Indeed, one clinical study showed that the mean ratio of umbilical cord glyburide concentration at delivery to maternal plasma glyburide concentration was ~0.7 (Hebert et al., 2009), indicating that a substantial amount of glyburide can cross the placenta to the fetus. Therefore, while total fetal exposure in human pregnancy is not known, there could be times following drug administration that fetal concentrations are nearly as high as maternal plasma concentrations. While the current dosage of glyburide is safe for use during pregnancy, dosage increases based on gestational age could raise concerns for fetal safety. In addition, since BCRP expression in human placenta decreases from ~28 weeks of gestation towards term (Meyer zu Schwabedissen et al., 2006), increased fetal exposure to glyburide in late pregnancy would be expected and may pose a safety concern that conflicts with the consideration to increase glyburide doses during pregnancy for improved maternal efficacy.

In summary, we have demonstrated gestational age-dependent maternal-fetal glyburide PK in pregnant mice. Results of this study suggest the possible need for increased glyburide

dosages even in early pregnancy should the same PK changes occur in humans, and that the pregnant mouse is an appropriate animal model to study glyburide disposition during pregnancy.

Acknowledgements

The authors would like to thank Dr. Laura Shireman for her advice regarding the implementation of the generalized estimating-equation (GEE) approach and her overall contribution to the statistical rigor of this work.

Authorship Contributions

Participated in research design: Shuster, Shen, Thummel, Hebert, and Mao

Conducted Experiments: Shuster and Risler

Contributed new reagents or analytic tools: Risler and Liang

Performed Data Analysis: Shuster, Risler, Liang, and Rice

Wrote or contributed to the writing of the manuscript: Shuster, Mao, Shen, Rice, Liang, Thummel, and Hebert

References

(2001) ACOG Practice Bulletin. Clinical management guidelines for obstetrician-gynecologists. Number 30, September 2001 (replaces Technical Bulletin Number 200, December 1994). Gestational diabetes. *Obstet Gynecol* **98:**525-538.

(2002) The Hyperglycemia and Adverse Pregnancy Outcome (HAPO) Study. *Int J Gynaecol Obstet* **78:**69-77.

Aleksunes LM, Cui Y, and Klaassen CD (2008) Prominent expression of xenobiotic efflux transporters in mouse extraembryonic fetal membranes compared with placenta. *Drug metabolism and disposition: the biological fate of chemicals* **36:**1960-1970.

Anderson GD (2005) Pregnancy-induced changes in pharmacokinetics: a mechanistic-based approach. *Clin Pharmacokinet* **44:**989-1008.

Balant L, Fabre J, Loutan L, and Samimi H (1979) Des 4-trans-hydroxy-glibenclamide show hypoglycemic activity? *Arzneimittelforschung* **29:**162-163.

Feghali MN and Mattison DR (2011) Clinical therapeutics in pregnancy. *J Biomed Biotechnol* **2011:**783528.

Gedeon C, Anger G, Lubetsky A, Miller MP, and Koren G (2008a) Investigating the potential role of multi-drug resistance protein (MRP) transporters in fetal to maternal glyburide efflux in the human placenta. *J Obstet Gynaecol* **28:**485-489.

Gedeon C, Anger G, Piquette-Miller M, and Koren G (2008b) Breast cancer resistance protein: mediating the trans-placental transfer of glyburide across the human placenta. *Placenta* **29:**39-43.

Gedeon C, Behravan J, Koren G, and Piquette-Miller M (2006) Transport of glyburide by placental ABC transporters: implications in fetal drug exposure. *Placenta* **27:**1096-1102.

Halekoh U, Hojsgaard S, and Yan J (2006) The R Package geepack for Generalized Estimating Equations. *J Stat Softw* **15:**1-11.

Hebert MF, Easterling TR, Kirby B, Carr DB, Buchanan ML, Rutherford T, Thummel KE, Fishbein DP, and Unadkat JD (2008) Effects of pregnancy on CYP3A and P-glycoprotein activities as measured by disposition of midazolam and digoxin: a University of Washington specialized center of research study. *Clin Pharmacol Ther* **84:**248-253.

Hebert MF, Ma X, Naraharisetti SB, Krudys KM, Umans JG, Hankins GD, Caritis SN, Miodovnik M, Mattison DR, Unadkat JD, Kelly EJ, Blough D, Cobelli C, Ahmed MS, Snodgrass WR, Carr DB, Easterling TR, and Vicini P (2009) Are we optimizing gestational diabetes treatment with glyburide? The pharmacologic basis for better clinical practice. *Clin Pharmacol Ther* **85:**607-614.

Hemauer SJ, Patrikeeva SL, Nanovskaya TN, Hankins GD, and Ahmed MS (2010) Role of human placental apical membrane transporters in the efflux of glyburide, rosiglitazone, and metformin. *Am J Obstet Gynecol* **202:**383 e381-387.

Jovanovic L and Pettitt DJ (2001) Gestational diabetes mellitus. *JAMA* **286:**2516-2518.

Klieger C, Pollex E, Kazmin A, and Koren G (2009) Hypoglycemics: pharmacokinetic considerations during pregnancy. *Ther Drug Monit* **31:**533-541.

Langer O, Conway DL, Berkus MD, Xenakis EM, and Gonzales O (2000) A comparison of glyburide and insulin in women with gestational diabetes mellitus. *N Engl J Med* **343:**1134-1138.

Mager H and Goller G (1998) Resampling methods in sparse sampling situations in preclinical pharmacokinetic studies. *J Pharm Sci* **87:**372-378.

Mathias AA, Hitti J, and Unadkat JD (2005) P-glycoprotein and breast cancer resistance protein expression in human placentae of various gestational ages. *Am J Physiol Regul Integr Comp Physiol* **289:**R963-969.

Metzger BE, Buchanan TA, Coustan DR, de Leiva A, Dunger DB, Hadden DR, Hod M, Kitzmiller JL, Kjos SL, Oats JN, Pettitt DJ, Sacks DA, and Zoupas C (2007) Summary and recommendations of the Fifth International Workshop-Conference on Gestational Diabetes Mellitus. *Diabetes Care* **30 Suppl 2:**S251-260.

Meyer zu Schwabedissen HE, Grube M, Dreisbach A, Jedlitschky G, Meissner K, Linnemann K, Fusch C, Ritter CA, Volker U, and Kroemer HK (2006) Epidermal growth factor-mediated activation of the map kinase cascade results in altered expression and function of ABCG2 (BCRP). *Drug Metab Dispos* **34:**524-533.

Nanovskaya TN, Nekhayeva I, Hankins GD, and Ahmed MS (2006) Effect of human serum albumin on transplacental transfer of glyburide. *Biochem Pharmacol* **72:**632-639.

Naraharisetti SB, Kirby BJ, Hebert MF, Easterling TR, and Unadkat JD (2007) Validation of a sensitive LC-MS assay for quantification of glyburide and its metabolite 4-transhydroxy glyburide in plasma and urine: an OPRU Network study. *J Chromatogr B Analyt Technol Biomed Life Sci* **860:**34-41.

Paglia MJ and Coustan DR (2011) Gestational diabetes: evolving diagnostic criteria. *Curr Opin Obstet Gynecol* **23:**72-75.

Paine MF, Khalighi M, Fisher JM, Shen DD, Kunze KL, Marsh CL, Perkins JD, and Thummel KE (1997) Characterization of interintestinal and intraintestinal variations in human CYP3A-dependent metabolism. *J Pharmacol Exp Ther* **283:**1552-1562.

R Core Team (2014) R: A language and environment for statistical computing, R Foundation for Statistical Computing, Vienna, Austria.

Ravindran S, Zharikova OL, Hill RA, Nanovskaya TN, Hankins GD, and Ahmed MS (2006) Identification of glyburide metabolites formed by hepatic and placental microsomes of humans and baboons. *Biochem Pharmacol* **72:**1730-1737.

Rydberg T, Jonsson A, Roder M, and Melander A (1994) Hypoglycemic activity of glyburide (glibenclamide) metabolites in humans. *Diabetes Care* **17:**1026-1030.

Shuster DL, Bammler TK, Beyer RP, Macdonald JW, Tsai JM, Farin FM, Hebert MF, Thummel KE, and Mao Q (2013) Gestational age-dependent changes in gene expression of metabolic enzymes and transporters in pregnant mice. *Drug Metab Dispos* **41:**332-342.

Thummel KE, Kharasch ED, Podoll T, and Kunze K (1993) Human liver microsomal enflurane defluorination catalyzed by cytochrome P-450 2E1. *Drug Metab Dispos* **21:**350-357.

Wang H, Wu X, Hudkins K, Mikheev A, Zhang H, Gupta A, Unadkat JD, and Mao Q (2006) Expression of the breast cancer resistance protein (Bcrp1/Abcg2) in tissues from pregnant mice: effects of pregnancy and correlations with nuclear receptors. *Am J Physiol Endocrinol Metab* **291:**E1295-1304.

Westfall PH and Young SS (1993) *Resampling-based multiple testing : examples and methods for P-value adjustment*. Wiley, New York.

Yan J and Fine J (2004) Estimating equations for association structures. *Stat Med* **23:**859-874.

Zhang H, Wu X, Wang H, Mikheev AM, Mao Q, and Unadkat JD (2008) Effect of pregnancy on cytochrome P450 3a and P-glycoprotein expression and activity in the mouse: mechanisms, tissue specificity, and time course. *Mol Pharmacol* **74:**714-723.

Zharikova OL, Fokina VM, Nanovskaya TN, Hill RA, Mattison DR, Hankins GD, and Ahmed MS (2009) Identification of the major human hepatic and placental enzymes responsible for the biotransformation of glyburide. *Biochem Pharmacol* **78:**1483-1490.

Zhou L, Naraharisetti SB, Liu L, Wang H, Lin YS, Isoherranen N, Unadkat JD, Hebert MF, and Mao Q (2010a) Contributions of human cytochrome P450 enzymes to glyburide metabolism. *Biopharm Drug Dispos* **31:**228-242.

Zhou L, Naraharisetti SB, Wang H, Unadkat JD, Hebert MF, and Mao Q (2008) The breast cancer resistance protein (Bcrp1/Abcg2) limits fetal distribution of glyburide in the pregnant mouse: an Obstetric-Fetal Pharmacology Research Unit Network and University of Washington Specialized Center of Research Study. *Mol Pharmacol* **73:**949-959.

Zhou L, Zhang Y, Hebert MF, Unadkat JD, and Mao Q (2010b) Increased glyburide clearance in the pregnant mouse model. *Drug Metab Dispos* **38:**1403-1406.

Figure Legends

Figure 1. Maternal plasma concentration-time profiles of glyburide in wild-type FVB pregnant mice throughout gestation. Mice were administered 20 µg of glyburide per mouse by retro-orbital injection. Data from gestation day 0 (gd 0) (solid circles), gd 7.5 (open squares), gd 10 (solid triangles), gd 15 (solid diamonds), and gd 19 (open diamonds) are shown as mean ± S.D. (n = 3-5 mice per time point). The main figure shows a semilogarithmic plot and the insert in the upper right-hand corner shows a rectilinear plot (including data from 5 – 240 min). Non-pregnant mice are referred to as gd 0.

Figure 2. Maternal plasma concentration-time profiles of metabolites M1-M3 in wild-type FVB pregnant mice throughout gestation. **A**, M1; **B**, M2a; **C**, M2b; **D**, M3. Data from gestation day 0 (gd 0) (solid circles), gd 7.5 (open squares), gd 10 (solid triangles), gd 15 (solid diamonds), and gd 19 (open diamonds) are shown as mean ± S.D. (n = 3-5 mice per time point). Non-pregnant mice are referred to as gd 0.

Figure 3. Fetal glyburide concentration-time profiles and fetal-to-maternal plasma concentration ratios in mid-late gestation. Data from gestation day (gd) 15 (open diamonds) and gd 19 (solid diamonds) are shown as mean ± S.D. (n = 20-40 fetuses per time point). **A**, semilogarithmic plot of fetal glyburide concentration over time; **B**, fetal to maternal plasma glyburide concentration ratios. Statistically significant differences in fetal concentrations and fetal-to-maternal plasma concentration ratios between gd 15 and 19 were determined using a generalized estimating-equation (GEE) approach with an independent correlation structure. *P*-

values were adjusted for multiple testing using a Bonferroni correction assuming a significance level of 0.05. * $p < 0.05$; ** $p < 0.01$; *** $p < 0.001$.

Figure 4. Gestational age-dependent depletion kinetics of glyburide in mouse liver microsomes. **A**, semilogarithmic plot of glyburide depletion over time in mouse liver microsomes. Data from gestation day 0 (gd 0) (solid circles), gd 7.5 (open squares), gd 10 (solid triangles), gd 15 (solid diamonds), and gd 19 (open diamonds) are shown as mean ± S.D. (n = 4-6 livers per gd). **B**, gestational age-dependent changes in glyburide CL_{int}. Shown are mean ± S.D. (n = 4-6 livers per gd). Statistically significant differences between gd 0 and gd 7.5, 10, 15 or 19, as indicated by an asterisk (*), were determined by the Kruskal-Wallis test followed by the Dunn's Multiple Comparison test assuming a significance level of 0.05. Non-pregnant mice are referred to as gd 0.

Footnotes:

This study was supported in part by the Eunice Kennedy Shriver National Institute of Child Health & Human Development (NICHD) [Grant U10HD047892], the National Center for Advancing Translational Sciences (NCATS), NIH [Grant TL1 RR025016], and the National Institutes of Health Pharmacological Sciences Training Grant [Grant T32 GM 007750]. The content is solely the responsibility of the authors and does not necessarily represent the official views of NICHD, NCATS or NIH. Diana Shuster is the recipient of the American Foundation for Pharmaceutical Education Pre-doctoral Fellowship in Pharmaceutical Sciences.

Table 1. Gestational age-dependent pharmacokinetics of glyburide in maternal plasma using a two-compartmental model

Parameter	Gd 0		Gd 7.5			Gd 10			Gd 15			Gd 19		
	Mean	**± SD or (95% CI)**	**Mean**	**± SD or (95% CI)**	***p***	**Mean**	**± SD or (95% CI)**	***p***	**Mean**	**± SD or (95% CI)**	***p***	**Mean**	**± SD or (95% CI)**	***p***
$AUC_{0\text{-}240\ min}$ ($\mu g \cdot min \cdot ml^{-1}$)	47.9	(40.5-54.1)	**37.2**	**(30.6-42.1)**	**0.021**	**29.5**	**(23.1-35.0)**	**0.002**	**20.7**	**(16.1-26.3)**	**0.001**	**21.2**	**(16.3-25.5)**	**0.001**
CL ($ml \cdot min^{-1}$)	0.42	(0.37-0.49)	**0.54**	**(0.48-0.65)**	**0.025**	**0.68**	**(0.57-0.87)**	**0.003**	**0.97**	**(0.76-1.24)**	**0.025**	**0.94**	**(0.79-1.23)**	**0.020**
CL_{bw} ($ml \cdot min^{-1} \cdot g^{-1}$)	0.018	(0.016-0.021)	**0.022**	**(0.020-0.027)**	**0.038**	**0.026**	**(0.022-0.033)**	**0.010**	**0.030**	**(0.024-0.039)**	**0.036**	**0.028**	**(0.023-0.036)**	**0.030**
Vc (ml)	2.1	(1.7-5.2)	4.0	(2.4-32.9)	0.124	3.9	(1.7-56.3)	0.205	5.2	(2.7-50.2)	0.137	3.5	(1.8-8.7)	0.398
$Vc_{,\ bw}$ ($ml \cdot g^{-1}$)	0.09	(0.07-0.22)	0.17	(0.10-1.33)	0.143	0.15	(0.07-2.24)	0.240	0.161	(0.084-1.630)	0.310	0.102	(0.052-0.254)	0.837
V_{β} (ml)	35.5	(29.1-48.3)	43.7	(34.7-57.0)	0.219	**68.8**	**(51.7-103.3)**	**0.012**	**89.9**	**(67.2-152)**	**0.039**	**93.6**	**(65.0-170)**	**0.030**
$V_{\beta,\ bw}$ ($ml \cdot g^{-1}$)	1.51	(1.24-2.06)	1.82	(1.45-2.37)	0.270	**2.61**	**(1.95-3.93)**	**0.023**	2.81	(2.10-4.84)	0.089	2.73	(1.92-4.88)	0.146
V_{ss} (ml)	21.2	(18.2-27.1)	29.2	(23.2-41.2)	0.067	**39.8**	**(28.3-61.7)**	**0.014**	**56.2**	**(38.4-84.6)**	**0.013**	**49.3**	**(33.3-71.5)**	**0.014**
$V_{ss,\ bw}$ ($ml \cdot g^{-1}$)	0.90	(0.77-1.15)	1.22	(0.97-1.71)	0.090	**1.51**	**(1.09-2.31)**	**0.033**	1.75	(1.20-2.69)	0.052	1.44	(0.98-2.13)	0.135
A ($ng \cdot ml^{-1}$)	9020	(3432-11154)	4602	(454-7999)	0.150	4851	(250-11317)	0.210	3680	(251-7316)	0.155	5556	(1565-10891)	0.280
α (min^{-1})	0.67	(0.38-0.83)	0.60	(0.20-0.84)	0.600	0.68	(0.19-0.98)	0.939	0.84	(0.18-1.35)	0.750	0.82	(0.37-1.28)	0.657
B ($ng \cdot ml^{-1}$)	431	(325-543)	382	(283-462)	0.465	**243**	**(169-299)**	**0.007**	**189**	**(127-238)**	**0.023**	**159**	**(93-216)**	**0.020**
β (min^{-1})	0.012	(0.009-0.014)	0.012	(0.01-0.014)	0.712	0.010	(0.007-0.012)	0.287	0.011	(0.006-0.015)	0.756	0.010	(0.006-0.013)	0.558
MBRT (min^{-1})	50.8	(44.9-59.3)	54.3	(46.7-64.4)	0.532	58.7	(48.3-72.9)	0.288	58.1	(43.0-75.5)	0.548	52.2	(40.8-63.7)	0.870
F_u (%)	2.19	± 0.25	2.45	± 0.67	0.394	2.27	± 0.59	0.766	2.00	± 0.11	0.260	2.27	± 0.52	0.741
Body Wt (g)	24	± 2.2	24	± 1.2		26	± 1.7		32	± 2.3		34	± 4.7	

Data reported as mean ± SD or (95% confidence interval). PK parameters on gd 7.5, 10, 15 or 19 with statistically significant ($p < 0.05$) differences versus gd 0 were bolded. Gd, gestation day; bw, body weight normalized; D, dose; AUC, area under the concentration-time curve;

CL, clearance; V, volume of distribution; MBRT, mean body residence time; f_u, fraction unbound ; *p*-values, *p*. Fraction unbound data are shown as mean ± S.D. from 6 maternal plasma samples for each gestation day, with duplicate determinations for each maternal plasma sample. Body weight data are means ± SD from n ≈ 30 mice per gestation day.

Table 2. Gestational age-dependent AUCs of glyburide and metabolites in maternal plasma using non-compartmental analyses

Parameter	Gd 0		Gd 7.5			Gd 10			Gd 15			Gd 19		
	Mean	**(95% CI)**	**Mean**	**(95% CI)**	***p***	**Mean**	**(95% CI)**	***p***	**Mean**	**(95% CI)**	***p***	**Mean**	**(95% CI)**	***p***
GLY AUC_{0-240} ($ng \cdot min \cdot ml^{-1}$)	55169	(46859-65378)	**39729**	**(32827-46781)**	**0.013**	**29308**	**(25112-33771)**	**<0.001**	**25302**	**(19276-31635)**	**<0.001**	**24216**	**(19689-30361)**	**<0.001**
M1 AUC_{0-240} ($ng \cdot min \cdot ml^{-1}$)	251	(204-294)	187	(156-219)	0.084	232	(205-258)	0.596	**129**	**(88-172)**	**0.006**	**141**	**(114-163)**	**0.011**
M2a AUC_{0-240} ($ng \cdot min \cdot ml^{-1}$)	359	(305-401)	**221**	**(166-265)**	**0.001**	**256**	**(206-295)**	**0.007**	**101**	**(61-149)**	**<0.001**	**131**	**(97-169)**	**<0.001**
M2b AUC_{0-240} ($ng \cdot min \cdot ml^{-1}$)	238	(208-274)	**159**	**(134-188)**	**0.009**	**141**	**(112-177)**	**0.005**	**47**	**(30-63)**	**<0.001**	**83**	**(66-99)**	**<0.001**
M3 AUC_{0-240} ($ng \cdot min \cdot ml^{-1}$)	251	(223-285)	**188**	**(148-237)**	**0.044**	**137**	**(107-170)**	**0.002**	**50**	**(32-67)**	**<0.001**	**70**	**(57-82)**	**<0.001**
M1/GLY AUC Ratio (%)	0.44	(0.37-0.51)	0.46	(0.37-0.55)	0.793	**0.77**	**(0.67-0.88)**	**<0.001**	0.49	(0.36-0.64)	0.534	0.57	(0.43-0.69)	0.091
M2a/GLY AUC Ratio (%)	0.63	(0.53-0.71)	0.54	(0.40-0.67)	0.270	**0.85**	**(0.70-0.98)**	**0.028**	**0.39**	**(0.25-0.55)**	**0.036**	0.53	(0.38-0.70)	0.298
M2b/GLY AUC Ratio (%)	0.42	(0.35-0.48)	0.39	(0.32-0.47)	0.576	0.47	(0.37-0.57)	0.485	**0.18**	**(0.12-0.24)**	**0.003**	0.33	(0.25-0.42)	0.231
M3/GLY AUC Ratio (%)	0.44	(0.37-0.51)	0.46	(0.36-0.60)	0.767	0.45	(0.36-0.55)	0.867	**0.19**	**(0.13-0.25)**	**0.003**	**0.28**	**(0.21-0.35)**	**0.041**

Data are reported as mean (95% confidence interval). Parameters on gd 7.5, 10, 15 or 19 with statistically significant ($p < 0.05$) differences versus gd 0 were bolded. The metabolite to glyburide AUC ratios were corrected for differences in the molarity between glyburide (494 $g \cdot mol^{-1}$) and metabolites (510 $g \cdot mol^{-1}$). Gd, gestation day; AUC, area under the concentration-time curve; *p*-values (*p*).

Table 3. Gestational age-dependent maternal-fetal AUCs of glyburide using non-compartmental analyses

Parameter	Gd 15		Gd 19		
	Mean	**(95% CI)**	**Mean**	**(95% CI)**	***p***
Maternal $AUC_{0\text{-}240\ min}$ ($ng \cdot min \cdot ml^{-1}$)	26129	(20129 - 32478)	24216	(19576 - 30273)	0.657
Fetal $AUC_{0\text{-}240\ min}$ ($ng \cdot min \cdot g^{-1}$)	462	(349 - 529)	**905**	**(726 - 1013)**	**<0.001**
Fetal/Maternal AUC Ratio (%)	1.8	(1.4 - 2.2)	**3.7**	**(2.8 - 4.6)**	**0.007**

Data reported as mean (95% confidence interval). Statistically significant ($p < 0.05$) differences between gd 19 and 15 were bolded. Gd, gestation day; AUC, area under the concentration-time curve; *p*-values (*p*).

Figure 1

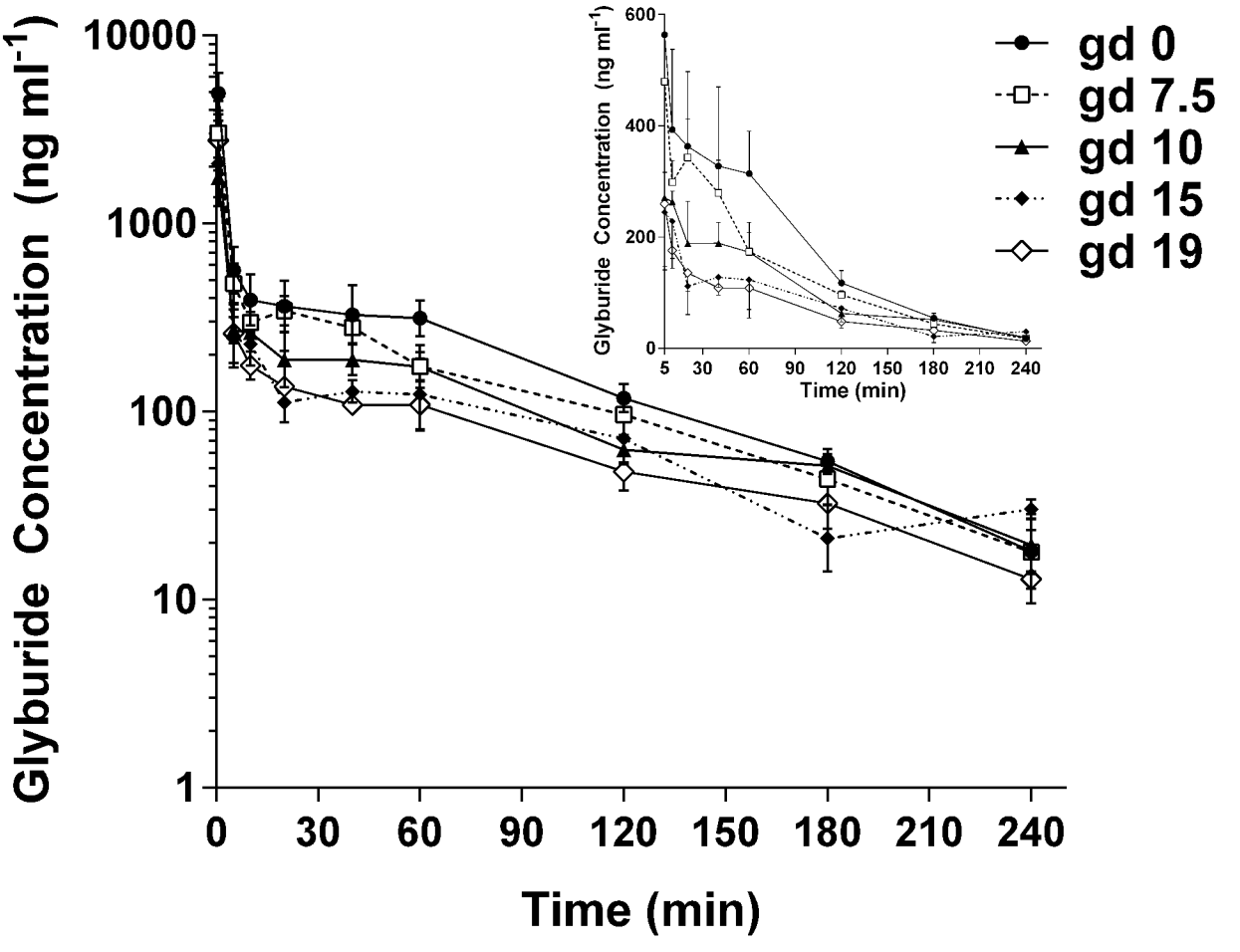
Glyburide Concentration (ng ml-1)
10000
1000
100
10
1
0
30
60
90
120
150
180
210
240
Time (min)
gd 0
gd 7.5
gd 10
gd 15
gd 19
Glyburide Concentration (ng ml-1)
600
400
200
0
5
30
60
90
120
150
180
210
240
Time (min)

Figure 2

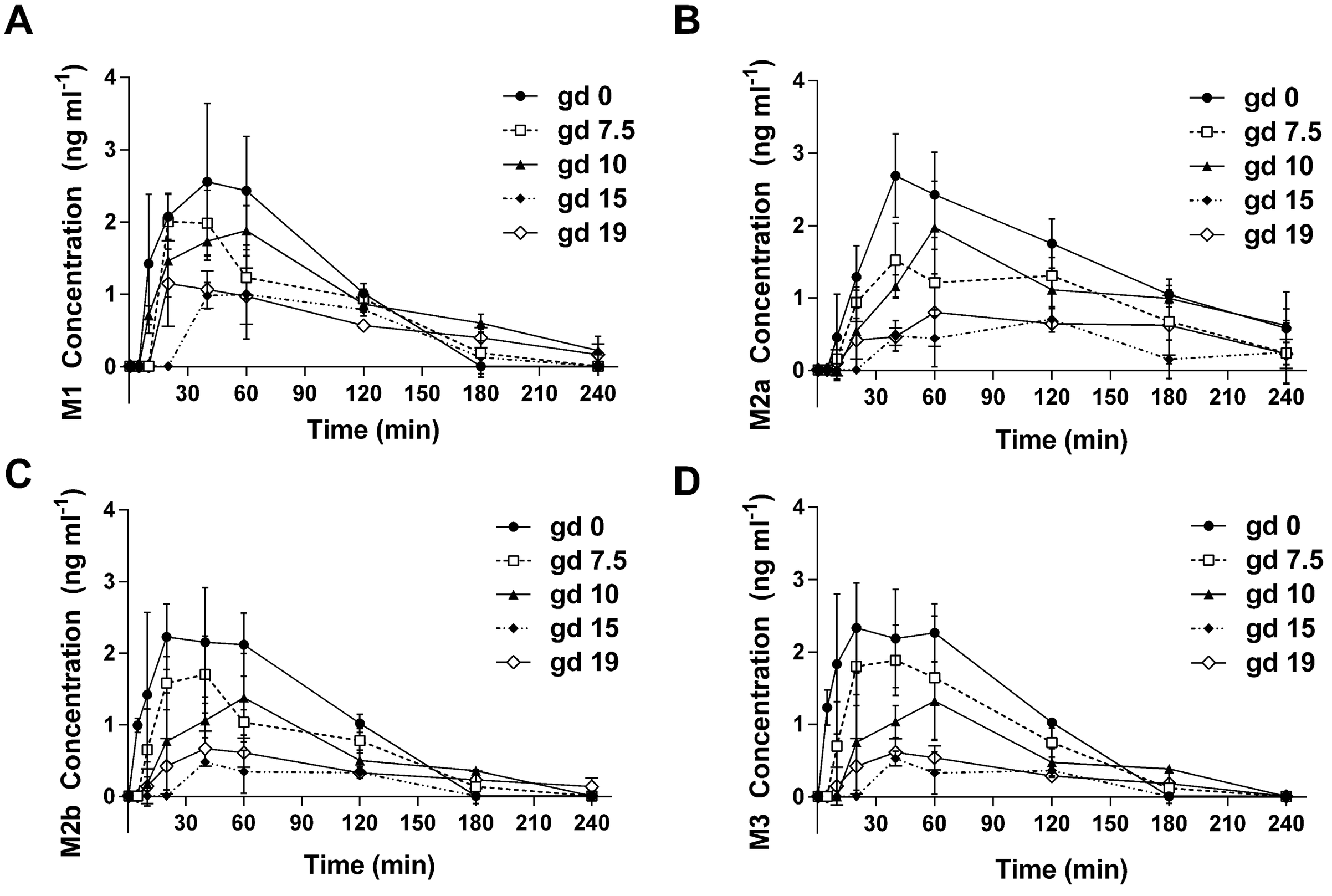
A
M1 Concentration (ng ml-1)
Time (min)
gd 0
gd 7.5
gd 10
gd 15
gd 19
B
M2a Concentration (ng ml-1)
Time (min)
gd 0
gd 7.5
gd 10
gd 15
gd 19
C
M2b Concentration (ng ml-1)
Time (min)
gd 0
gd 7.5
gd 10
gd 15
gd 19
D
M3 Concentration (ng ml-1)
Time (min)
gd 0
gd 7.5
gd 10
gd 15
gd 19

Figure 3

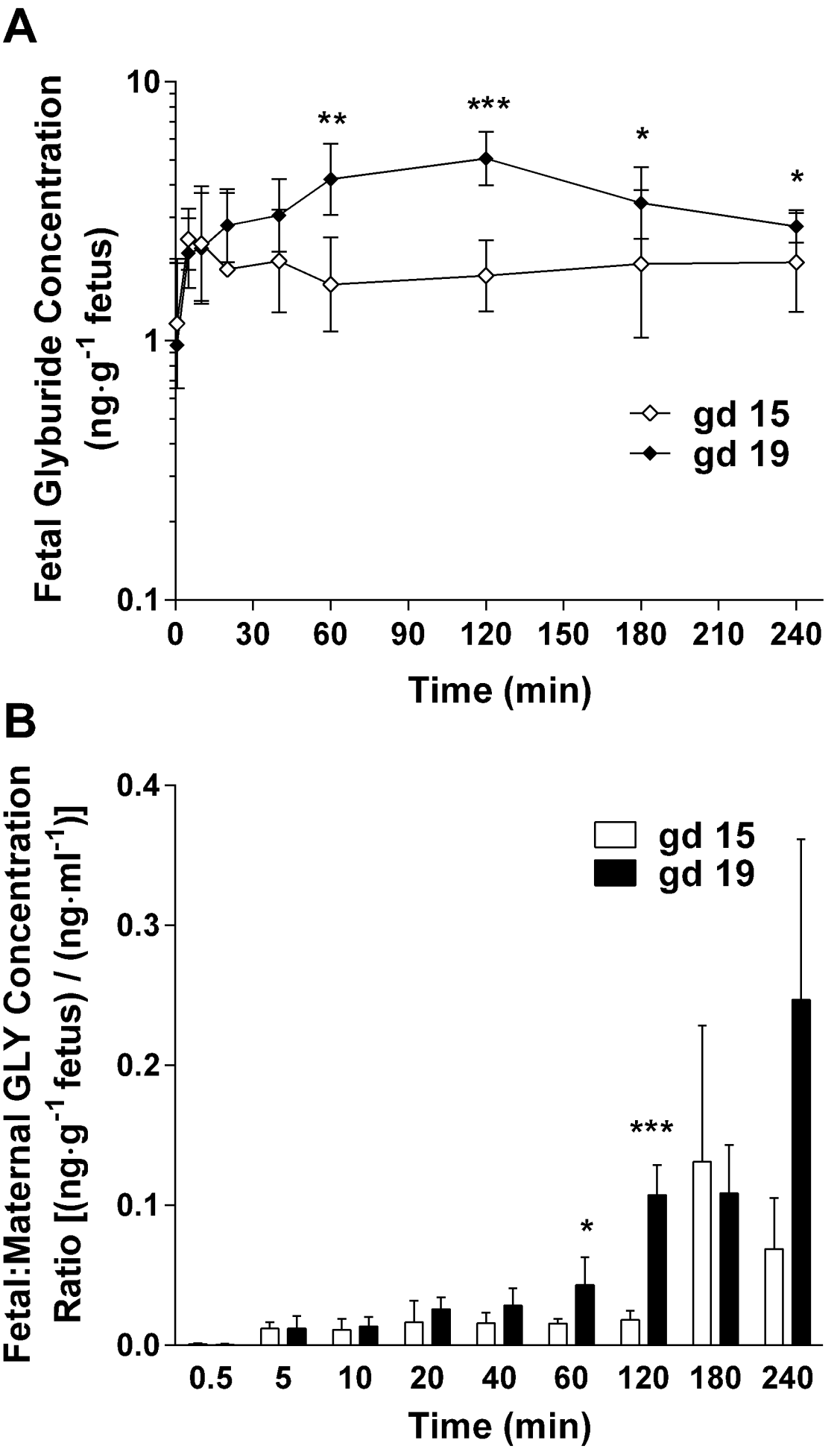
A
Fetal Glyburide Concentration (ng·g-1 fetus)
10
1
0.1
**
***
*
*
gd 15
gd 19
0
30
60
90
120
150
180
210
240
Time (min)
B
Fetal:Maternal GLY Concentration Ratio [(ng·g-1 fetus) / (ng·ml-1)]
0.4
0.3
0.2
0.1
0.0
gd 15
gd 19
*
***
0.5
5
10
20
40
60
120
180
240
Time (min)

Figure 4

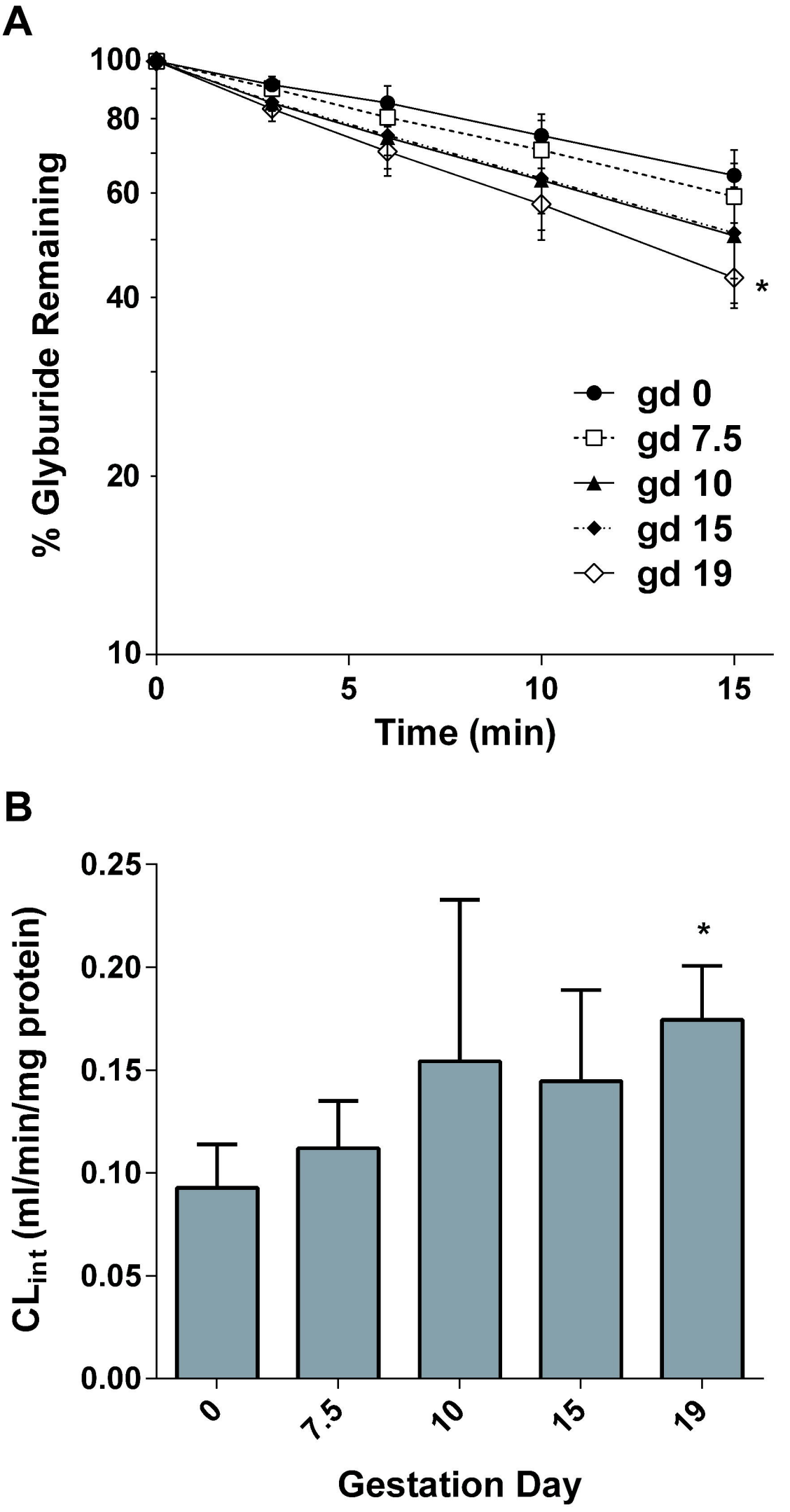
A
100
80
60
40
20
10
% Glyburide Remaining
0
5
10
15
Time (min)
*
gd 0
gd 7.5
gd 10
gd 15
gd 19
B
0.25
0.20
0.15
0.10
0.05
0.00
CLint (ml/min/mg protein)
*
0
7.5
10
15
19
Gestation Day